Journal of Nuclear Medicine, published on December 7, 2017 as doi:10.2967/jnumed.117.199406

# Sex as a Biological Variable in Preclinical Imaging Research: Initial Observations with $^{18}$F-Fluorothymidine

Szeman Ruby Chan[1*], Kelley Salem[2], Justin Jeffery[3], Ginny L. Powers[2**], Yongjun Yan[2,4], Kooresh I. Shoghi[5], Aparna M. Mahajan[6], Amy M. Fowler[2,3,4]

[1]Department of Pathology and Immunology, Washington University School of Medicine, St. Louis, MO 63110

[2]Department of Radiology, University of Wisconsin School of Medicine and Public Health, 600 Highland Avenue, Madison, WI 53792

[3]University of Wisconsin Carbone Cancer Center, 600 Highland Avenue, Madison, WI 53792.

[4]Department of Medical Physics, University of Wisconsin School of Medicine and Public Health, 1111 Highland Avenue, Madison, WI 53705

[5]Mallinckrodt Institute of Radiology, Washington University School of Medicine, St. Louis, MO 63110

[6]Department of Pathology and Laboratory Medicine, University of Wisconsin School of Medicine and Public Health, 1685 Highland Avenue, Madison, WI 53705

[*]Current affiliation: Janssen Pharmaceutical Companies of Johnson & Johnson, 1400 McKean Road, Spring House, PA 19477

[**]Current affiliation: Kendrick Labs Inc., 1202 Ann Street, Madison, WI 53713

**First Author Contact Information:** Szeman Ruby Chan, PhD, 1400 McKean Road, Spring House, PA 19477; Phone: 215-540-4023; Fax: 215-540-4763; E-mail: schan31@ITS.JNJ.com

**Corresponding Author Information:** Amy M. Fowler, MD, PhD, 600 Highland Avenue, Madison, WI 53792-3252, USA. Phone: 608-262-9186; (Fax): 608-265-1836; Email: afowler@uwhealth.org

**Financial support:** This work was supported by grants from the NCI (U01CA141541-01) and Mallinckrodt Institute of Radiology at Washington University (MIR 11-037). K.I.S. is supported by U24CA209837 and U54CA199092. Funding was also provided to A.M.F. by the UW Institute of Clinical and Translational Research KL2 Scholar Award (5KL2TR000428-09, 4KL2TR000428-10), School of Medicine and Public Health, and the Department of Radiology.

**Running title:** Sexual dimorphism in preclinical imaging

**Word count:** 4941

**Abstract**

The study objective was to investigate whether sex influences 3'-deoxy-3'-[$^{18}$F]fluorothymidine ($^{18}$F-FLT) uptake and tissue distribution in mouse models of cancer.

**Methods:** $^{18}$F-FLT biodistribution was measured in three strains of male and female mice (129S6/SvEv, athymic nude, and BALB/c). $^{18}$F-Fluoro-2-deoxy-2-D-glucose ($^{18}$F-FDG) biodistribution was performed for comparison. $^{18}$F-FLT uptake was also measured in female 129S6/SvEv mice bearing estrogen-dependent SSM3 mouse mammary tumors, male athymic nude mice bearing androgen-dependent CWR22 prostate cancer xenografts, and male and female athymic nude mice bearing estrogen-independent MDA-MB-231 human breast cancer xenografts. Ki67 expression was assayed by immunohistochemistry. Positron emission tomography/computed tomography (PET/CT) imaging was performed to visualize $^{18}$F-FLT biodistribution and for pharmacokinetics.

**Results:** Greater $^{18}$F-FLT activity was observed in blood, liver, muscle, heart, kidney, and bone in female mice compared to males. Pharmacokinetic analysis demonstrated early increased renal $^{18}$F-FLT activity and greater accumulation of $^{18}$F-FLT in the urinary bladder in male mice compared with females. The differential pattern of $^{18}$F-FLT biodistribution between the sexes seen with $^{18}$F-FLT was not observed with $^{18}$F-FDG. Increased tumoral $^{18}$F-FLT uptake compared with muscle was observed in both the SSM3 mammary tumors (2.4±0.17 vs 1.6±0.14%ID/g at 2 h post-injection, p=0.006) and CWR22 prostate cancer xenografts (0.34±0.08 vs 0.098±0.033%ID/g at 2 h post-injection, p=0.03). However, due to higher nonspecific muscle uptake in female mice, tumor-to-muscle (T:M) uptake ratios were greater for CWR22 tumors compared with SSM3 tumors (4.2±0.78 vs 1.5±0.049 at 2 h post-injection, p=0.008). Sex-dependent differences in $^{18}$F-FLT uptake was also observed for MDA-MB-231

xenografts (T:M ratios 7.2±0.9 female vs 16.9±8.6 male; p=0.039) . Conversely, greater tumoral Ki67 staining was observed in female mice (71±3% female vs 54±2% male; p=0.009) which more closely matched the relative differences in absolute $^{18}$F-FLT tumor uptake values (4.5±0.99%ID/g female vs 1.9±0.30%ID/g male; p=0.03).

**Conclusion:** Depending on whether female or male mice are used, differences in biodistribution and nonspecific tissue uptake can adversely impact quantitative measures of $^{18}$F-FLT uptake. Thus, sex is a potential variable to consider in defining quantitative imaging metrics using $^{18}$F-FLT to assess tumor proliferation.

**Keywords:**

1. 3'-deoxy-3'-[$^{18}$F]fluorothymidine
2. Cancer
3. Sex differences
4. Positron emission tomography
5. Mice

## Introduction

A rising concern from the National Institutes of Health is the importance of including sex as a biological variable in animal studies and human clinical trials (*1*). Women were not required to be included as subjects in clinical research until the Revitalization Act of 1993. However, consideration of sex as an experimental variable did not extend to federally-funded preclinical work until 2014. This policy is part of a broader goal to increase reproducibility and transparency between research studies and to ensure scientific rigor.

Often times, the sex of cell lines are not considered in experimental design since the canonical thought was that, on the molecular level, basic cellular processes transcends gender differences. While basic molecular mechanisms may be similar, male and female cells may respond differently to various stimuli. For example, it was shown that male neurons are more sensitive to oxidative stress than female neurons (*2*). Sex differences also extend to the organismal level with sexual dimorphism identified in approximately 57% of phenotypes in mice (*3*). Thus, sex is an important biological variable to consider in the design, analysis, and reporting of preclinical research. This concept is especially pertinent for understanding the pathophysiology and treatment of diseases that affect both genders, like many forms of cancer.

One of the hallmarks of cancer is abnormal sustained proliferation (*4*). As more therapies emerge and the field of precision medicine matures, imaging tools that can detect biological change prior to anatomic tumor size changes are becoming increasingly important. The most studied radiopharmaceutical for *in vivo* imaging of cell proliferation is 3'-deoxy-3'-[$^{18}$F]fluorothymidine ($^{18}$F-FLT) (*5*,*6*). It enters cells via membrane nucleoside transporters and undergoes phosphorylation by the cytosolic thymidine kinase-1 enzyme as part of the thymidine salvage pathway of DNA synthesis during S-phase of the cell cycle. Unlike endogenous

thymidine, phosphorylated $^{18}$F-FLT does not incorporate into DNA and due to a relatively slow rate of dephosphorylation, it accumulates intracellularly (*7*).

Positron emission tomography (PET) imaging using $^{18}$F-FLT is being studied as a non-invasive method to measure the proliferative capacity of cancer and may provide an early indication of treatment response (*5,6*). While not yet approved by the U.S. Food and Drug Administration, $^{18}$F-FLT has been studied through clinical trials in over 1,000 individuals and in patients with multiple cancer types (*8*). Biologic variables that can affect $^{18}$F-FLT uptake include plasma thymidine levels, the expression level and functional activity of thymidine kinase-1, thymidylate synthase, and nucleoside transporters, and the overall balance of *de novo* versus salvage pathways of thymidine utilization (*9*). This study aimed to determine whether sex influences $^{18}$F-FLT uptake and tissue biodistribution in preclinical oncology models.

## Materials and Methods

### Cell lines, mice, and tumor implantation

Experiments were carried out under an approved biosafety protocol. The human estrogen receptor (ER) negative breast cancer cell line, MDA-MB-231, was cultured at 37 °C and 10% $CO_2$ in Dulbecco's Modified Eagle Medium (Corning; Corning, NY) with high glucose containing 10% fetal bovine serum (Corning; Corning, NY) with penicillin and streptomycin (Gibco; Waltham, MA). SSM1 and SSM3 cell lines were isolated from primary spontaneous mammary adenocarcinomas in female transgenic STAT1$^{-/-}$ mice and were maintained in culture as described previously (*10*). The prostate cancer xenograft model, CWR22, was created from primary prostate carcinoma in a man with metastatic prostate cancer and was maintained *in vivo* via serial transplantation (*11,12*). All cell lines tested negative for murine pathogens and were

negative for Mycoplasma contamination which can affect uptake of thymidine analogues (*13*). Cell line authentication was performed using short tandem repeat analysis.

Experiments were carried out according to the American Association for Laboratory Animal Science guidelines under an approved protocol by the Animal Studies Committees and performed in AAALAC-accredited specific pathogen-free facilities at Washington University School of Medicine (St. Louis, MO) and the University of Wisconsin-Madison (Madison, WI). Mice aged 6 to 8 weeks were injected subcutaneously with $1x10^6$ SSM1 or SSM3 cells in 100 µL phosphate buffered saline or $2x10^6$ MDA-MB-231 cells in 50% Matrigel (BD Biosciences; San Jose, CA) by volume into the right thoracic mammary fat pad. Tumor growth was monitored by palpation and measured in two perpendicular dimensions with calipers. Tumor volumes were calculated using the formula $\boldsymbol{a \times b^2/2}$, where **a** is the long diameter and **b** is the short diameter.

**Radiopharmaceuticals, PET/CT imaging, and tissue biodistribution assay**

$^{18}$F-FLT and $^{18}$F-Fluoro-2-deoxy-2-D-glucose ($^{18}$F-FDG) were synthesized by the Cyclotron Facility at Washington University (*14,15*). $^{18}$F-FLT specific activity at the end of synthesis ranged from 59-225 GBq/µmol (1606-6068 mCi/µmol). $^{18}$F-FLT was also provided by the UW-Madison Radiopharmaceutical Production Facility. Specific activity at the end of synthesis ranged from 333-629 GBq/µmol (9000-17000 mCi/µmol). Radiochemical purity was 100% for all preparations.

For PET/CT imaging, non-fasted mice were injected via tail vein with approximately 0.93 MBq (25 µCi) of $^{18}$F-FLT. Mice were not anesthetized during the radiotracer uptake period. Mice anesthetized with 1.5-2.0% isoflurane were scanned supine in a small animal PET/CT scanner (Inveon, Siemens Preclinical Solutions, Knoxville, TN) 1 hour following

injection. CT images were acquired for approximately 12 minutes followed by PET image acquisition (40 million counts - typically less than 10 minutes). One male and one female mouse were positioned side-by-side and imaged simultaneously for each scan. Images were analyzed using Inveon Research Workplace 3.0 (Siemens Medical Solutions USA, Inc., Malvern, PA). The reconstruction method used was 3D ordered subset expectation maximization/maximum a posteriori with attenuation correction. The binning protocol for dynamic acquisitions were 1frx3sec, 6frx2sec, 9frx5sec, 6frx10sec, 4frx30sec, 2frx60sec, 2frx120sec, and 22frx300sec. PET and CT images were automatically co-registered and adjusted if needed via visual alignment in all three planes. Regions of interest (ROI) were manually drawn around the tumor and within triceps muscle for non-target tissue uptake using CT images for visual anatomic localization. Additional ROIs were drawn around the kidneys, urinary bladder, bone (femur), liver, and heart for blood activity. Data are expressed as mean percent injected dose per gram (% ID/g). Tumor-to-muscle (T:M) ratio was calculated as the ratio of % ID/g of tumor to that of muscle. $^{18}$F-FLT clearance from the blood was calculated using a one phase exponential decay equation of the time-activity curve.

For biodistribution assays, tissues (blood, liver, muscle, heart, kidney, and whole bone) were harvested 1 or 2 hours after tail vein injection of approximately 0.74-0.89 MBq (20-24 μCi) of $^{18}$F-FLT or 0.74 MBq (20 μCi) of $^{18}$F-FDG in non-fasted mice. Radioactivity was measured using a gamma counter (2480 Wizard$^2$, Perkin Elmer; Waltham, MA) and decay-corrected in order to calculate % ID/g. To minimize differences due to variations in $^{18}$F-FLT preparations, the same batch of $^{18}$F-FLT was used for experimentation within the same species of male and female mice.

**Statistical analyses**

Results are presented as mean±standard error unless indicated elsewise. Two-way ANOVA with a Sidak post-test was used to determine significance between male and female mice for biodistribution assays. The Mann-Whitney test was used to determine the statistical significance between control and experimental groups. Paired t test was implemented to compare across different time points within the same group of animals. All tests are two-sided with a p value $\leq 0.05$ considered significant. Analyses were performed using GraphPad Prism, version 6.05 (GraphPad Software, La Jolla, CA).

**Results**

**Comparison of $^{18}$F-FLT tissue biodistribution in female versus male mice**

To determine whether sex is a potential biological variable for $^{18}$F-FLT uptake in preclinical models of cancer, we performed tissue biodistribution experiments using three different mouse strains, 129S6/SvEv, athymic nude, and BALB/c (**Fig. 1**). $^{18}$F-FLT activity was higher at 1 and 2 h post injection in the blood, liver, muscle, heart, and bone in female 129S6/SvEv mice compared to males (**Fig. 1A**). At 1 h, there was similar renal accumulation of $^{18}$F-FLT in both sexes. At 2 h, $^{18}$F-FLT activity measured in the kidneys of female mice was less than in males. For athymic nude mice, females had greater $^{18}$F-FLT uptake in all tissues measured compared to males with the exception of bone at 1 h, which was not significantly different (**Fig. 1B**). The third mouse strain tested, BALB/c, showed significantly increased $^{18}$F-FLT uptake in all female organs measured compared to males (**Fig. 1C**). Sex-dependent differences in $^{18}$F-FLT tissue biodistribution were accentuated when results were normalized to mouse weight (**Supplemental Fig. 1**). Thus, we observed increased $^{18}$F-FLT uptake in the

blood, liver, muscle, heart, and bone of females compared with males across all three mouse strains.

To test whether these differences in tissue biodistribution could be visualized with PET imaging, female and male athymic nude mice were chosen as a representative strain and underwent $^{18}$F-FLT PET/CT imaging. Female mice had greater overall visual $^{18}$F-FLT signal compared to males with the exception of the kidneys and urinary bladder which appeared similar (**Fig. 2**). Therefore, PET/CT imaging is sensitive enough to detect sex differences in $^{18}$F-FLT biodistribution and further confirmed our data obtained via gamma counting of excised tissues.

**Dynamic $^{18}$F-FLT PET/CT imaging in female mice compared to male mice**

To investigate $^{18}$F-FLT pharmacokinetics in male and female mice, we performed dynamic PET/CT imaging of athymic nude mice at multiple time points during the first hour post injection (**Fig. 3**). Time-activity curves demonstrated that male mice had increased $^{18}$F-FLT activity in the urinary bladder at all time points compared to females (**Fig. 3A**). Male mice also had a greater spike in renal $^{18}$F-FLT uptake during the first 1-2 minutes post injection compared to females (**Fig. 3B**). For blood (**Fig. 3C**), liver (**Fig. 3D**), bone (**Fig. 3E**), and muscle (**Fig. 3F**), the time-activity curves appeared similar in male and female mice at early time points. The half-life of $^{18}$F-FLT in blood was 0.36 min (95%CI:0.29-0.47) for male mice and 0.20 min (95%CI:0.15-0.30) for females. However, the curves tended to diverge around 30 minutes post injection, and by 60 minutes activity in these tissues were higher in the female mice compared to males. This data suggests that there is a difference in the physiological processing of $^{18}$F-FLT during the first 30 minutes post injection.

**Comparison of $^{18}$F-FDG tissue biodistribution in female versus male mice**

To determine if sex variability is specific to $^{18}$F-FLT, we tested a more commonly used $^{18}$F-labeled radiopharmaceutical, $^{18}$F-FDG, for imaging glucose metabolism. A tissue biodistribution assay was performed in male and female 129S6/SvEv mice 1 and 2 h post injection using the same dose of $^{18}$F-FDG as performed previously with $^{18}$F-FLT (**Fig. 4**). We observed no significant difference in $^{18}$F-FDG tissue uptake except that female mice had greater uptake in the heart compared to male mice at both time points. Thus, with the exception of cardiac uptake, differential sex-dependent tissue biodistribution may be specific to $^{18}$F-FLT and may not pertain to all $^{18}$F-labeled molecular imaging agents.

**Comparison of $^{18}$F-FLT uptake by estrogen-dependent mouse mammary tumors to androgen-dependent prostate cancer xenografts**

Due to the physiological differences in $^{18}$F-FLT biodistribution and kinetics based on sex, we tested the potential impact of this difference for imaging proliferation of hormone-dependent tumor models in male and female mice. We used ER+ SSM3 tumors as a representative estrogen-dependent mammary tumor model grown in female mice and CWR22 tumors as a representative androgen-dependent prostate tumor model in which tumoral $^{18}$F-FLT uptake can be reduced by androgen ablation in male mice (*16*). SSM3 and CWR22 tumors were similar in size (mean±standard deviation 488 ±494 mm$^3$ and 272 ± 192 mm$^3$, respectively; p=0.21) at the time of assay. Tumor uptake of $^{18}$F-FLT was measured at 1 and 2 h post injection using tissue biodistribution assays. There was statistically significant tumoral $^{18}$F-FLT uptake compared with muscle uptake in both the SSM3 tumors (4.3±0.27 vs 3.2±0.25 %ID/g at 1h, p=0.02; 2.4±0.17 vs 1.6±0.14 %ID/g at 2 h post-injection, p=0.006) and CWR22 xenografts (0.86±0.06 vs 0.41±0.07

%ID/g, p=0.004 at 1h; 0.34±0.08 vs 0.098±0.033 %ID/g at 2 h post-injection, p=0.03). However due to higher nonspecific muscle uptake in female mice, T:M uptake ratios were greater for CWR22 xenografts compared with SSM3 tumors at both 1 h and 2 h post-injection (p=0.03 and 0.0083, respectively) (**Fig. 5**). The highest T:M ratio observed for the CWR22 xenografts was at 2 h post-injection and measured 4.2±0.78. The highest T:M ratio observed for the SSM3 tumors was at 2 h post-injection and measured only 1.5±0.05. As a result, CWR22 xenografts display more tumor-specific uptake of $^{18}$F-FLT based on their higher T:M uptake ratios; whereas SSM3 tumors exhibit higher absolute values of $^{18}$F-FLT uptake along with higher nonspecific muscle uptake. Another mouse mammary carcinoma cell line (SSM1) shows similar biodistribution results as SSM3 tumors grown in female 129S6/SvEv mice (**Supplemental Figure 2**).

**Comparison of $^{18}$F-FLT uptake by hormone-independent human breast cancer xenografts in female and male mice**

The mouse-derived SSM3 tumors require estrogen for tumor growth and were grown in female immunocompetent mice. The human-derived CWR22 tumors depend on androgens for tumor growth and were grown in male immunocompromised mice. Thus, we chose to directly compare $^{18}$F-FLT uptake of a hormone-independent breast cancer cell line that can be grown as xenografts in either female or male mice. MDA-MB-231 cells were grown as tumor xenografts in athymic nude female and male mice, injected with $^{18}$F-FLT, sacrificed 2 hours later and tissue harvested and counted for radioactivity. Tumor volumes were 499 ±143 mm$^3$ (mean±standard deviation) in the female mice and 352 ±104 mm$^3$ in male mice at the time of the biodistribution experiment (p=0.05). Both female and male mice had greater $^{18}$F-FLT uptake in MDA-MB-231 tumors compared to muscle (4.5±0.99 %ID/g female tumor vs 0.67±0.18 %ID/g muscle,

p=0.005; 1.9±0.30 %ID/g male tumor vs 0.16±0.07 %ID/g male muscle; p= 0.0004) (**Fig. 6A**). However, female mice also had more nonspecific muscle uptake compared to males (0.67±0.18 %ID/g vs 0.16±0.07 %ID/g; p=0.0275). This disparity resulted in a lower T:M ratio for female mice compared to males (7.2±0.9 vs 16.9±8.6; p=0.039).

To determine whether absolute tumor uptake (%ID/g) or T:M uptake ratio better reflects proliferation, tumor Ki67 staining was performed. A greater percentage of Ki67-positive staining was observed in MDA-MB-231 tumors grown in females (71±3%) compared to those grown in male mice (54±2%; p=0.009; **Fig. 6B**).

**Discussion**

The purpose of this study was to investigate whether sex is a potential biological variable in preclinical studies of $^{18}$F-FLT PET imaging. We demonstrated that female mice have overall greater $^{18}$F-FLT uptake in multiple tissues compared with males. We also observed increased $^{18}$F-FLT activity in the kidney at early time points and greater accumulation of $^{18}$F-FLT in the urinary bladder at all points in male mice compared with females suggesting sex-dependent differences in renal clearance. Differences in $^{18}$F-FLT biodistribution between sexes resulted in altered interpretation of proliferative status by imaging depending on whether absolute tumor uptake (%ID/g) or T:M ratio was used as the method of quantification for two hormone-dependent tumor model systems. When using the same hormone-independent breast cancer xenograft capable of being grown in both male and female mice, distinct patterns of $^{18}$F-FLT uptake in MDA-MB-231 xenografts were observed depending on the sex of the mouse. Furthermore, quantification of $^{18}$F-FLT uptake as absolute tumor uptake (%ID/g) better approximates the Ki67 proliferative index than T:M ratios. This work demonstrates that sex is

important to consider in defining quantitative imaging metrics using $^{18}$F-FLT as a noninvasive measure of tumor proliferation.

To the best of our knowledge, sex-dependent differences in $^{18}$F-FLT biodistribution and PET imaging of preclinical models has not been previously reported. In a systematic review of 174 primary publications using $^{18}$F-FLT for oncologic imaging, factors influencing $^{18}$F-FLT uptake in tumors were identified (*9*). These publications included tumor models grown in only male or female mice and lacked a direct comparison of $^{18}$F-FLT imaging between the sexes. Similarly, a comprehensive review of preclinical studies comparing $^{18}$F-FDG and $^{18}$F-FLT PET imaging for tumor response monitoring lacked information regarding whether any differences between sexes were investigated (*17*).

Our results add to a small, but growing, amount of literature determining how sex may impact preclinical imaging research. Some evidence points to differences due to pharmacokinetic properties of the imaging agent, such as absorption, distribution, metabolism, and excretion. For example, sex differences in metabolism and distribution of the opioid receptor ligand, N-(3-$^{18}$F-fluoropropyl)-N-nordiprenorphine, in rats have been reported (*18*). Other evidence reflects the underlying sex-dependent differences in expression level of the binding target/receptor of the imaging agent. Using a C-11 labeled PET radioligand for imaging sphingosine-1-phosphate receptor 2 in a mouse model of multiple sclerosis, differences in tracer uptake in the cerebellum between male and female mice was identified which reflected the underlying sex-dependent difference in receptor protein expression (*19,20*). Sex differences were also reported in sigma-2 receptor binding density in the brain of a transgenic mouse model of Alzheimer's disease using a sigma-2 receptor specific imaging agent (*21*).

Comparatively more reports regarding sex differences in clinical imaging research exist, particularly for neuro- and cardiac imaging. For example, several studies have reported gender differences in regional brain glucose metabolism using $^{18}$F-FDG PET and neuroreceptor imaging with targeted radioligands for opioid, dopamine, and cannabinoid receptors (*22-25*). Gender differences in cardiac glucose metabolism have also been demonstrated using $^{18}$F-FDG PET/CT in healthy men and women (*26*).

This study has several limitations. First, this initial report included only a few breast and prostate cancer models. Subsequent work using additional cell lines will establish the generalizability of the results. In addition to sex, age is another potential biologic variable in preclinical studies (*27*). While our results show sex differences in $^{18}$F-FLT biodistribution using only one age group (6-8 weeks) for xenograft studies, results may differ in older mice used for transgenic/spontaneous tumor model systems. Lastly, our results may not translate to humans due to species-level pharmacokinetic differences. In humans, $^{18}$F-FLT undergoes hepatic metabolism via glucuronidation (*28*), but is mainly excreted by the kidneys in its original form in mice (*29,30*). Furthermore, plasma thymidine levels have been shown to be 320-fold higher in rodents compared with humans (*31*).

**Conclusion**

Our results demonstrate that sex is an important variable to consider for preclinical imaging using $^{18}$F-FLT. Sex-dependent differences in $^{18}$F-FLT biodistribution and nonspecific tissue uptake can adversely impact quantitative measures of $^{18}$F-FLT uptake and conclusions regarding relative tumor proliferation status when comparing with *ex vivo* reference standards, such as Ki67 staining. These results have broader implications as the National Cancer Institute

and the imaging community have embarked on numerous initiatives to define imaging metrics of response to therapy. Thus, standardization between sexes to yield sex-independent imaging metrics of tumor phenotype and therapy response is critical to advance the translational utility of molecular imaging.

**Acknowledgments**

The authors thank Dr. John Katzenellenbogen for thoughtful discussions and critical reading of this manuscript. We also thank Nicole Fettig and the Washington University Pre-Clinical Imaging Facility staff for their excellent technical assistance. We thank the Washington University Cyclotron Facility and Carmen Dence for her expertise in $^{18}$F-FLT radiosynthesis and the UW-Madison Cyclotron Laboratory for $^{18}$F production. We also thank the UW Translational Research Initiatives in Pathology laboratory, in part supported by the UW Department of Pathology and Laboratory Medicine and University of Wisconsin Carbone Cancer Center (UWCCC) grant P30 CA014520, the Small Animal Imaging Facility and Experimental Pathology Laboratory (P30 CA014520) for use of its facilities and services.

**References**

**1.** Clayton JA, Collins FS. Policy: NIH to balance sex in cell and animal studies. *Nature.* 2014;509:282-283.

**2.** Du L, Bayir H, Lai Y, et al. Innate gender-based proclivity in response to cytotoxicity and programmed cell death pathway. *J Biol Chem.* 2004;279:38563-38570.

**3.** Karp NA, Mason J, Beaudet AL, et al. Prevalence of sexual dimorphism in mammalian phenotypic traits. *Nat Commun.* 2017;8:15475.

**4.** Hanahan D, Weinberg RA. Hallmarks of cancer: the next generation. *Cell.* 2011;144:646-674.

**5.** Bollineni VR, Kramer GM, Jansma EP, Liu Y, Oyen WJ. A systematic review on [(18)F]FLT-PET uptake as a measure of treatment response in cancer patients. *Eur J Cancer.* 2016;55:81-97.

**6.** Tehrani OS, Shields AF. PET imaging of proliferation with pyrimidines. *J Nucl Med.* 2013;54:903-912.

**7.** Grierson JR, Schwartz JL, Muzi M, Jordan R, Krohn KA. Metabolism of 3'-deoxy-3'-[F-18]fluorothymidine in proliferating A549 cells: validations for positron emission tomography. *Nucl Med Biol.* 2004;31:829-837.

**8.** Investigator's brochure for 3'-deoxy-3'-[F-18] fluorothymidine: [F-18]FLT: an investigational positron emission tomography (PET) radiopharmaceutical for injection intended for use as an in vivo diagnostic for imaging active cellular proliferation of malignant tumors. National Cancer Institute. https://www.acrin.org/portals/0/protocols/6688/flt_ib__final_v5-5-2011.pdf. Accessed 7/11/2017.

**9.** Schelhaas S, Heinzmann K, Bollineni VR, et al. Preclinical applications of 3'-deoxy-3'-[18F]fluorothymidine in oncology - a systematic review. *Theranostics.* 2017;7:40-50.

**10.** Chan SR, Vermi W, Luo J, et al. STAT1-deficient mice spontaneously develop estrogen receptor alpha-positive luminal mammary carcinomas. *Breast Cancer Res.* 2012;14:R16.

**11.** Wainstein MA, He F, Robinson D, et al. CWR22: androgen-dependent xenograft model derived from a primary human prostatic carcinoma. *Cancer Res.* 1994;54:6049-6052.

**12.** Pretlow TG, Wolman SR, Micale MA, et al. Xenografts of primary human prostatic carcinoma. *J Natl Cancer Inst.* 1993;85:394-398.

**13.** Sinigaglia F, Talmadge KW. Inhibition of [3H]thymidine incorporation by Mycoplasma arginini-infected cells due to enzymatic cleavage of the nucleoside. *Eur J Immunol.* 1985;15:692-696.

**14.** Suehiro M, Vallabhajosula S, Goldsmith SJ, Ballon DJ. Investigation of the role of the base in the synthesis of [18F]FLT. *Appl Radiat Isot.* 2007;65:1350-1358.

**15.** Yun M, Oh SJ, Ha HJ, Ryu JS, Moon DH. High radiochemical yield synthesis of 3'-deoxy-3'-[18F]fluorothymidine using (5'-O-dimethoxytrityl-2'-deoxy-3'-O-nosyl-beta-D-threo pentofuranosyl)thymine and its 3-N-BOC-protected analogue as a labeling precursor. *Nucl Med Biol.* 2003;30:151-157.

**16.** Oyama N, Ponde DE, Dence C, Kim J, Tai YC, Welch MJ. Monitoring of therapy in androgen-dependent prostate tumor model by measuring tumor proliferation. *J Nucl Med.* 2004;45:519-525.

**17.** Jensen MM, Kjaer A. Monitoring of anti-cancer treatment with (18)F-FDG and (18)F-FLT PET: a comprehensive review of pre-clinical studies. *Am J Nucl Med Mol Imaging.* 2015;5:431-456.

**18.** Chesis PL, Griffeth LK, Mathias CJ, Welch MJ. Sex-dependent differences in N-(3-[18F]fluoropropyl)-N-nordiprenorphine biodistribution and metabolism. *J Nucl Med.* 1990;31:192-201.

**19.** Yue X, Jin H, Liu H, Rosenberg AJ, Klein RS, Tu Z. A potent and selective C-11 labeled PET tracer for imaging sphingosine-1-phosphate receptor 2 in the CNS demonstrates sexually dimorphic expression. *Org Biomol Chem.* 2015;13:7928-7939.

**20.** Cruz-Orengo L, Daniels BP, Dorsey D, et al. Enhanced sphingosine-1-phosphate receptor 2 expression underlies female CNS autoimmunity susceptibility. *J Clin Invest.* 2014;124:2571-2584.

**21.** Sahlholm K, Liao F, Holtzman DM, Xu J, Mach RH. Sigma-2 receptor binding is decreased in female, but not male, APP/PS1 mice. *Biochem Biophys Res Commun.* 2015;460:439-445.

**22.** Hu Y, Xu Q, Li K, et al. Gender differences of brain glucose metabolic networks revealed by FDG-PET: evidence from a large cohort of 400 young adults. *PLoS One.* 2013;8:e83821.

**23.** Zubieta JK, Dannals RF, Frost JJ. Gender and age influences on human brain mu-opioid receptor binding measured by PET. *Am J Psychiatry.* 1999;156:842-848.

**24.** Okita K, Petersen N, Robertson CL, Dean AC, Mandelkern MA, London ED. Sex differences in midbrain dopamine D2-type receptor availability and association with nicotine dependence. *Neuropsychopharmacology.* 2016;41:2913-2919.

**25.** Normandin MD, Zheng MQ, Lin KS, et al. Imaging the cannabinoid CB1 receptor in humans with [11C]OMAR: assessment of kinetic analysis methods, test-retest reproducibility, and gender differences. *J Cereb Blood Flow Metab.* 2015;35:1313-1322.

**26.** Kakinuma Y, Okada S, Nogami M, Kumon Y. The human female heart incorporates glucose more efficiently than the male heart. *Int J Cardiol.* 2013;168:2518-2521.

**27.** Jackson SJ, Andrews N, Ball D, et al. Does age matter? The impact of rodent age on study outcomes. *Lab Anim.* 2017;51:160-169.

**28.** Shields AF, Briston DA, Chandupatla S, et al. A simplified analysis of [18F]3'-deoxy-3'-fluorothymidine metabolism and retention. *Eur J Nucl Med Mol Imaging.* 2005;32:1269-1275.

**29.** Kim SJ, Lee JS, Im KC, et al. Kinetic modeling of 3'-deoxy-3'-18F-fluorothymidine for quantitative cell proliferation imaging in subcutaneous tumor models in mice. *J Nucl Med.* 2008;49:2057-2066.

**30.** Barthel H, Cleij MC, Collingridge DR, et al. 3'-deoxy-3'-[18F]fluorothymidine as a new marker for monitoring tumor response to antiproliferative therapy in vivo with positron emission tomography. *Cancer Res.* 2003;63:3791-3798.

**31.** Li KM, Clarke SM, Rivory LP. Quantitation of plasma thymidine by high-perfomance liquid chromatography-atmospheric pressure chemical ionization mass spectrometry and its application to pharmadynamic studies in cancer patients. *Anal Chim Acta.* 2003;486:51-61.

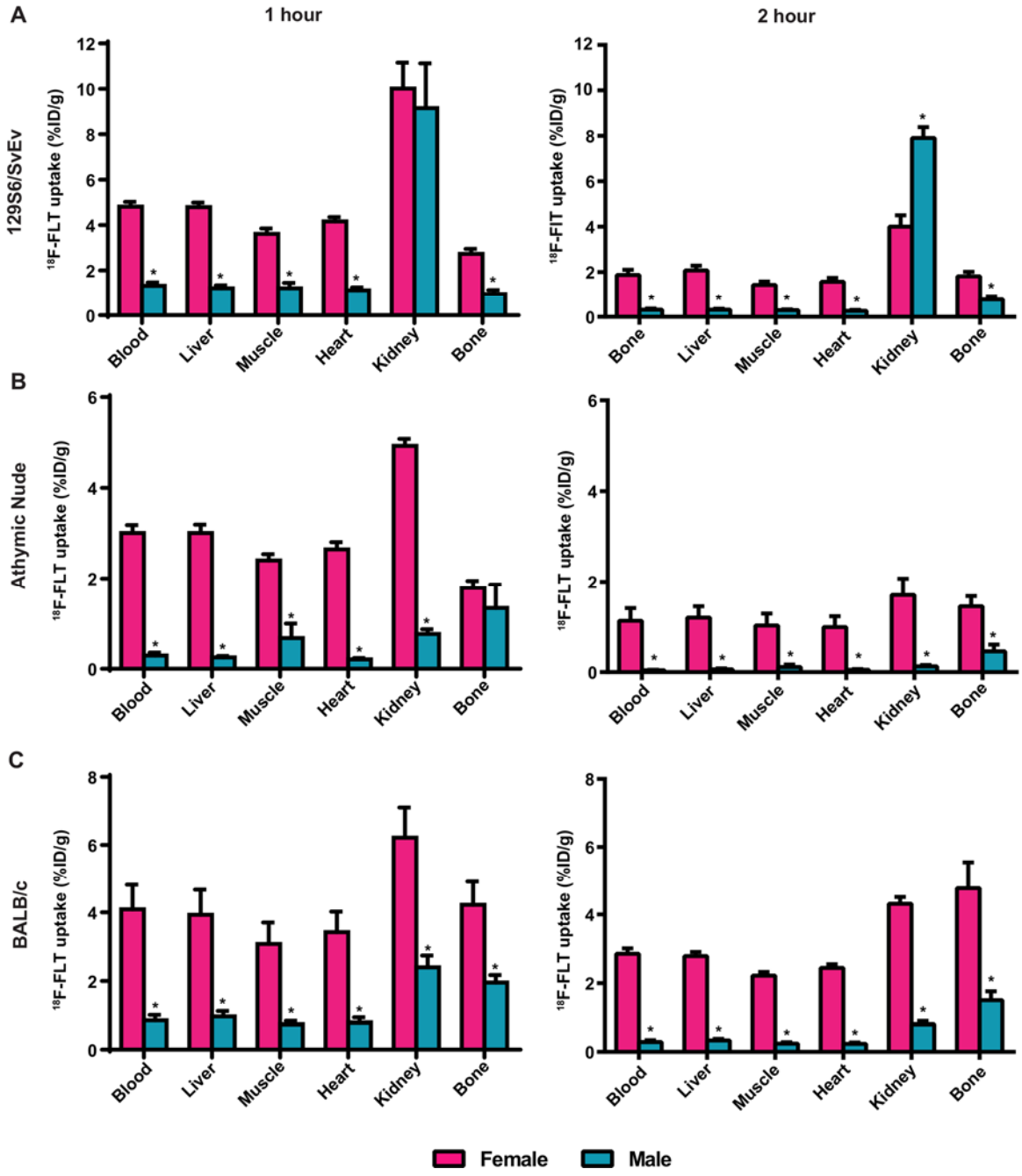


**Figure 1: $^{18}$F-FLT biodistribution in male and female mice.**

Male and female (**A**) 129S6/SvEv (**B**) athymic nude (**C**) and BALB/c mice were sacrificed 1 h and 2 h following injection of 0.74-0.89 MBq (20-24 µCi) $^{18}$F-FLT (n=5 129S6/SvEv; n=5 athymic nude; n=4 BALB/c per time point). Percent injected dose/gram (%ID/g) was calculated. * $p<0.05$ (male vs female for each tissue)

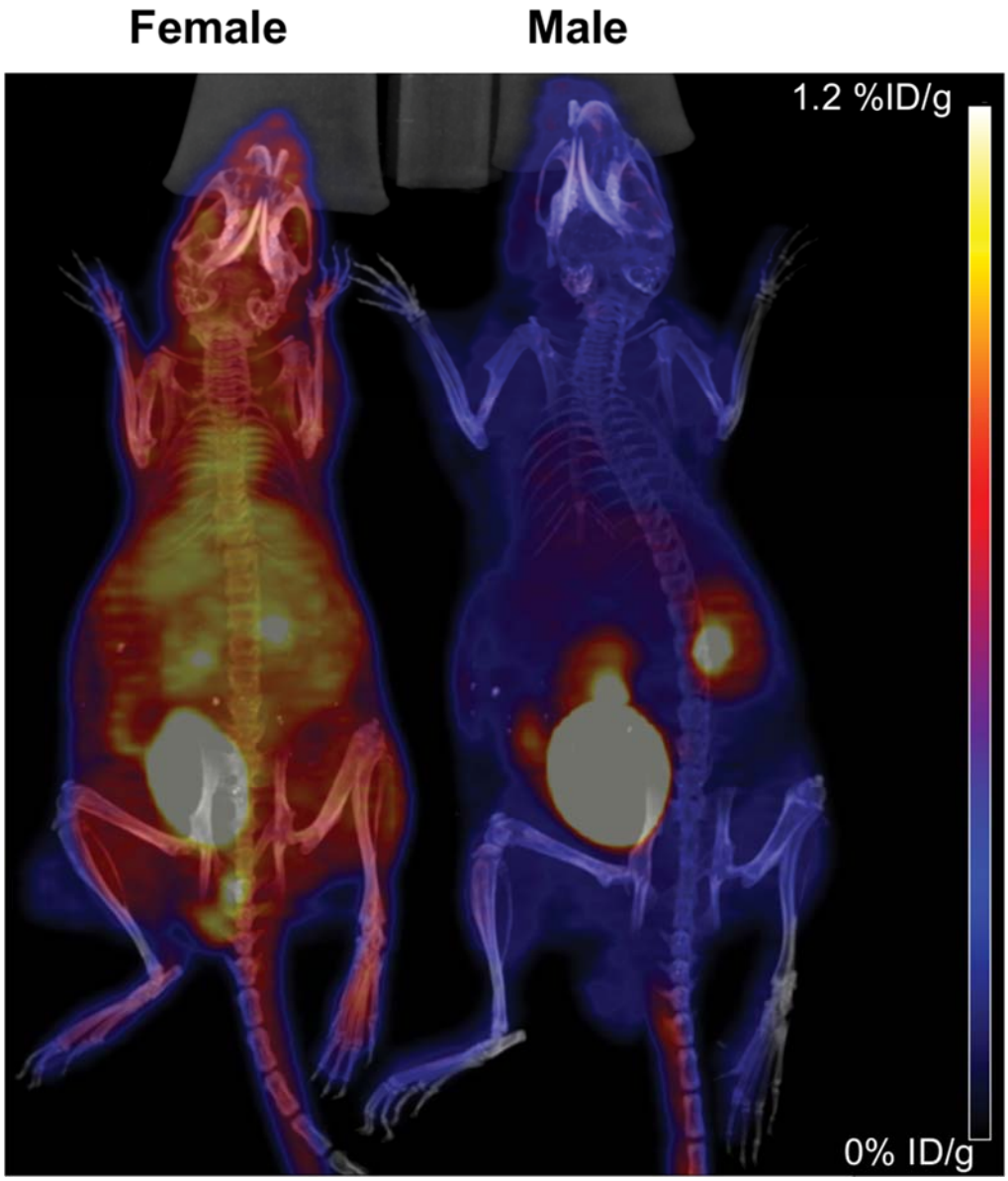


**Figure 2: $^{18}$F-FLT PET/CT imaging of male and female athymic nude mice.**

Maximal intensity projection fused PET and CT images of representative female (left; n=3) and male (right; n=3) mice scanned concurrently 1 h after injection of 0.93 MBq (25 μCi) $^{18}$F-FLT.

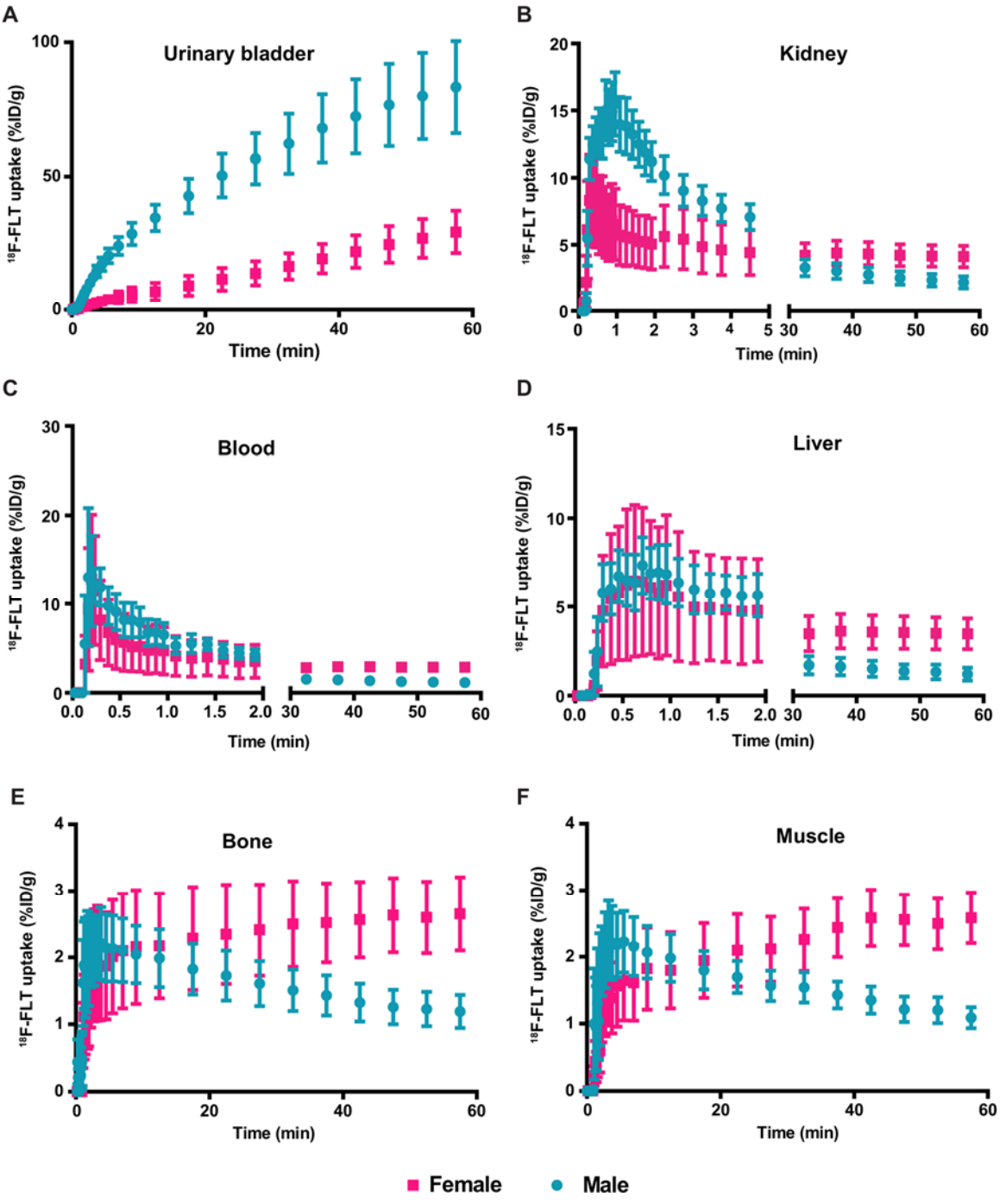


**Figure 3: Time-activity curves of $^{18}$F-FLT in male and female athymic nude mice.**

Male and female athymic nude mice were imaged using dynamic PET imaging acquisition from 0 to 60 minutes following injection of approximately 0.93 MBq (25 μCi) $^{18}$F-FLT. Regions of

interest were drawn and time-activity curves were determined for: (**A**) urinary bladder, (**B**) kidney, (**C**) blood, (**D**) liver, (**E**) bone, and (**F**) muscle.

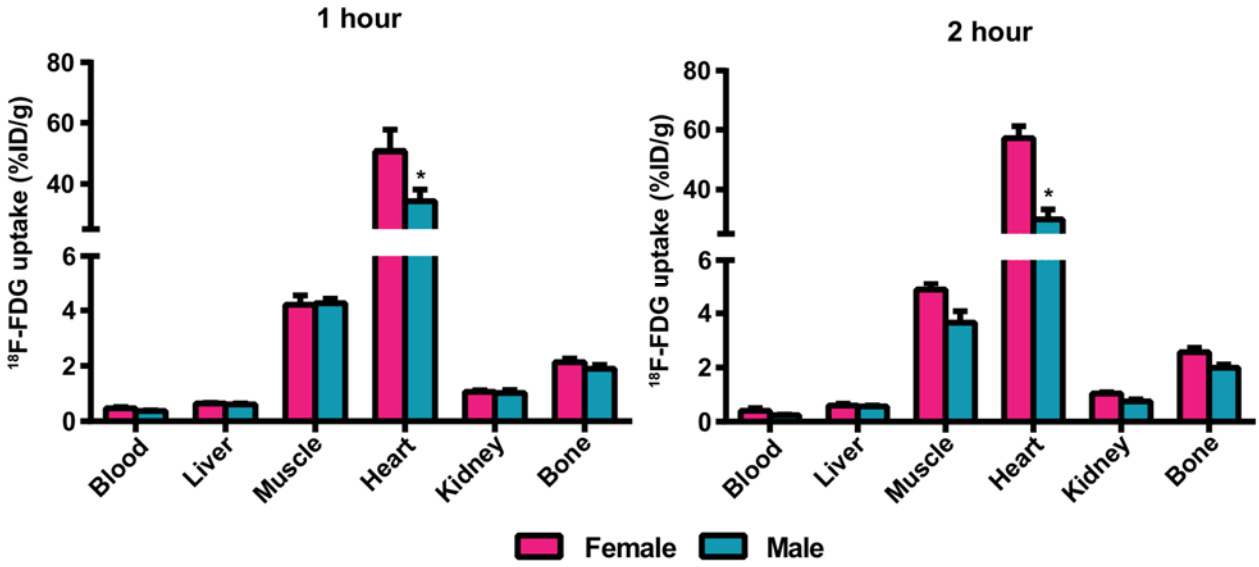


**Figure 4: $^{18}$F-FDG biodistribution in male and female 129S6/SvEv mice.**

Male and female 129S6/SvEV mice were sacrificed 1h and 2 h following injection of 0.74 MBq (20 µCi) $^{18}$F-FDG (n=5 per group). Percent injected dose/gram (%ID/g) was calculated. * $p<0.05$ (male vs female for each tissue)

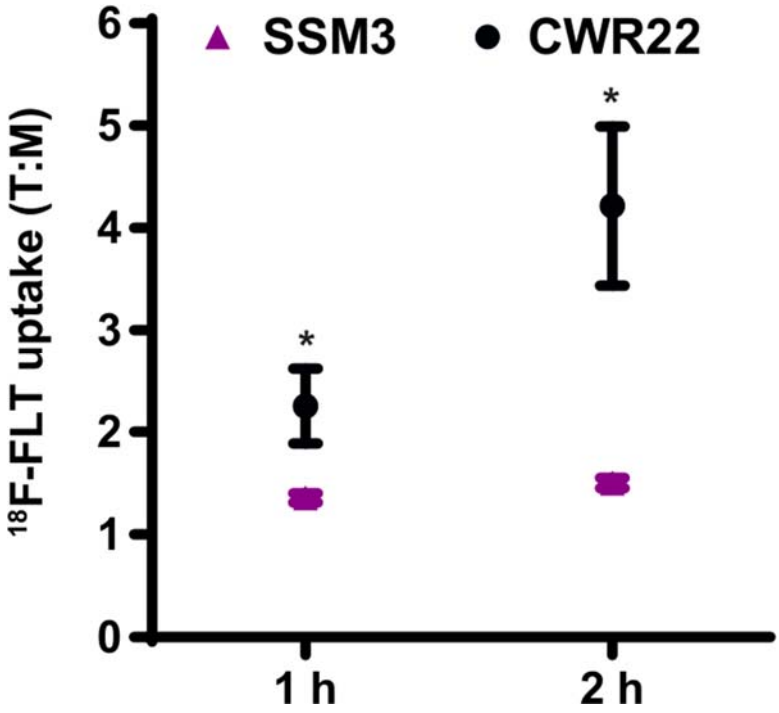


**Figure 5: $^{18}$F-FLT biodistribution in SSM3 mammary tumor-bearing and CWR22 prostate cancer xenograft-bearing mice.**

Mice bearing SSM3 or CWR22 tumors were sacrificed 1 h (n=5 SSM3; n=4 CWR22) and 2 h (n=5 SSM3; n=5 CWR22) after injection of 0.85 MBq (23 μCi) $^{18}$F-FLT. Percent injected dose/gram (%ID/g) of tumor and muscle were calculated. The ratios of %ID/g in tumor to %ID/g in muscle (T:M) were calculated. * $p<0.05$ (CWR22 vs SSM3 tumors)

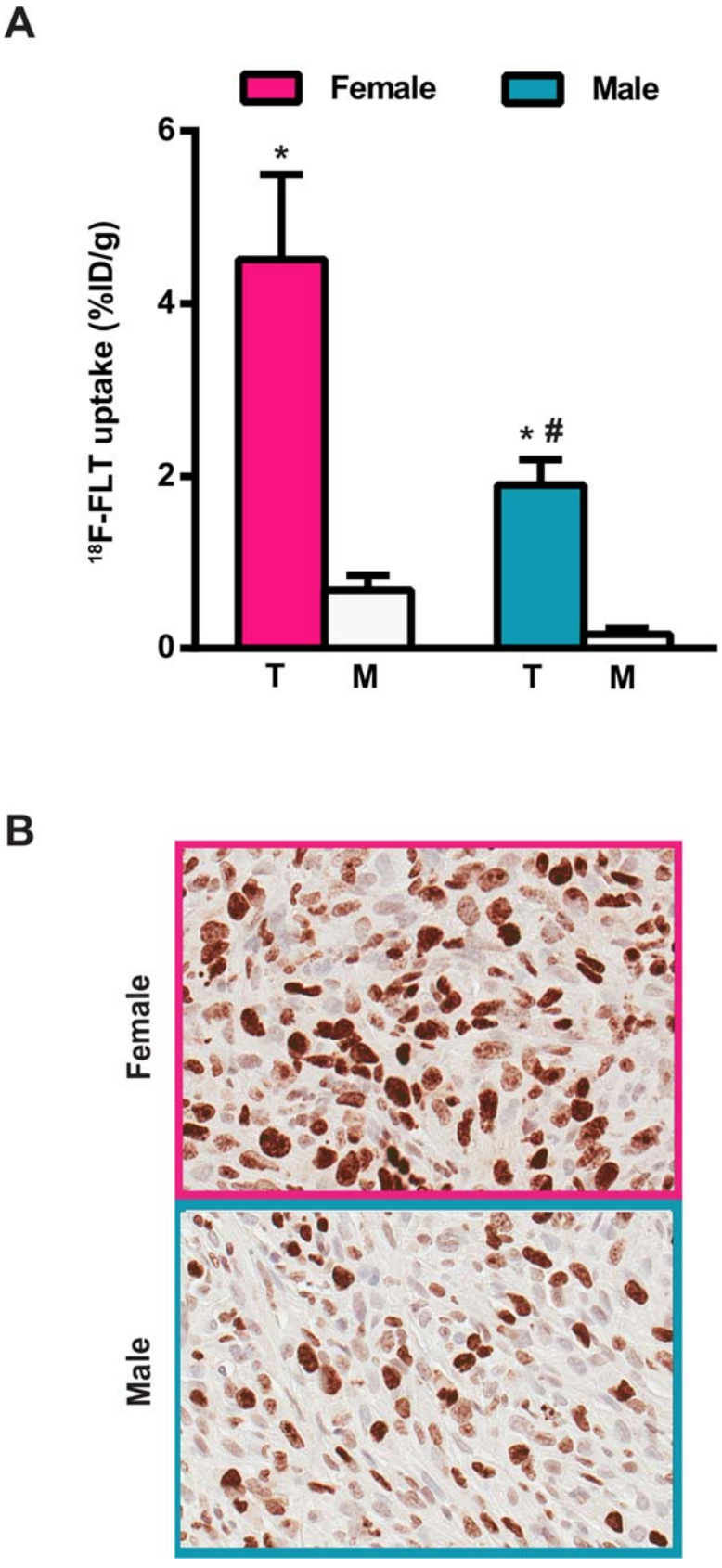


**Figure 6: $^{18}$F-FLT biodistribution in hormone-independent MDA-MB-231 breast cancer xenograft-bearing male and female mice.**

**(A)** Female (n=5) and male (n=5) mice bearing ER-negative MDA-MB-231 human breast cancer cells were sacrificed 2 h after 0.67-0.78 MBq (18-21 μCi) $^{18}$F-FLT injection. Percent injected dose/gram (%ID/g) of tumor (T) and muscle (M) were calculated. * $p<0.05$ (tumor vs muscle); # $p<0.05$ (female tumor vs male tumor). **(B)** Representative Ki67 immunohistochemistry of MDA-MB-231 tumors in female and male mice (40x).

## Supplemental Materials and Methods

### Mice

Athymic NCr-nu/nu mice were purchased from the National Cancer Institute-Frederick National Laboratory for Cancer Research Animal Production Program (Frederick, MD). Male mice were used for the CWR22 prostate cancer xenografts and female mice were used for the MDA-MB-231 human breast cancer xenografts. BALB/c mice were also purchased from NCI (Frederick, MD). Male and female 129S6/SvEv mice were purchased from Taconic Farms, Inc. (Hudson, NY). Female mice were used for the SSM1 and SSM3 mouse mammary tumor cell lines.

### Tissue histology

Sections of formalin-fixed paraffin-embedded mammary tumors were deparaffinized and rehydrated followed by antigen retrieval in citrate buffer (pH 6) and stained for Ki67 (VP-K452, 1:800; Vector Laboratories, Inc.; Burlingame, CA). Positive signal was developed using SignalStain® IHC Detection Reagent (HRP, mouse; Cell Signaling Technology; Danvers, MA) followed by diaminobenzidine chromogen. Hematoxylin and eosin staining was also performed. A whole-slide bright field imaging system (Leica Biosystems; Aperio Image Scope software; Wetzlar, Germany) was used to scan slides at 40x magnification. Percentage of tumor cells staining positive for Ki67 was visually scored by a pathologist with subspecialty training in breast pathology and 4 years of experience.

## Supplemental Figure Legends

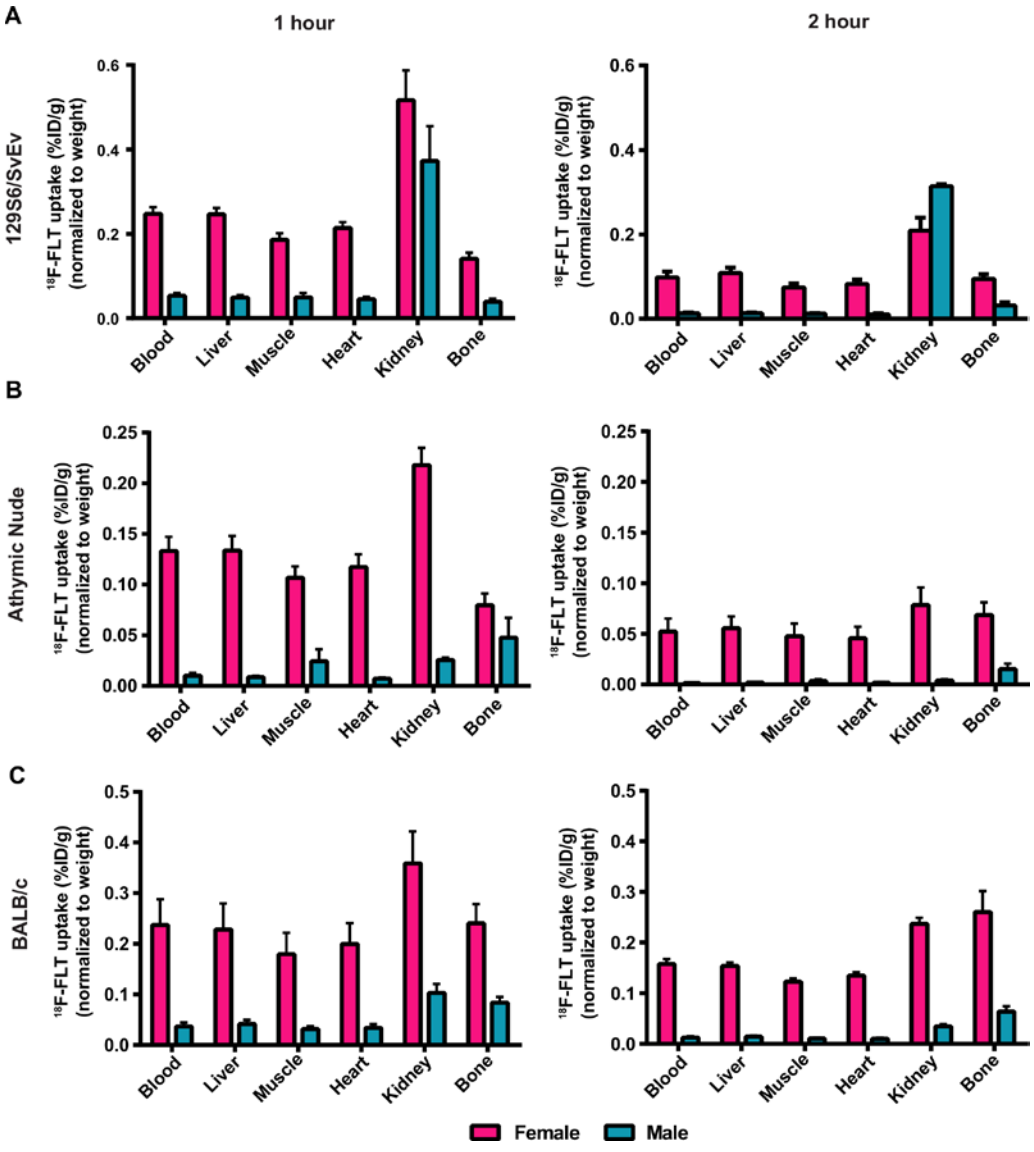


**Supplemental Figure 1: $^{18}$F-FLT biodistribution normalized to mouse weight.**

Male and female (**A**) 129S6/SvEv, (**B**) athymic nude, (**C**) and BALB/c mice were sacrificed 1 h and 2 h following injection of 0.74-0.89 MBq (20-24 µCi) $^{18}$F-FLT (n=5 129S6/SvEv; n=5 athymic nude; n=4 BALB/c per time point). Tissues were harvested, weighed, and radioactivity was measured by gamma counting. Percent injected dose/gram (%ID/g) of each tissue type was calculated and normalized to mouse weight.

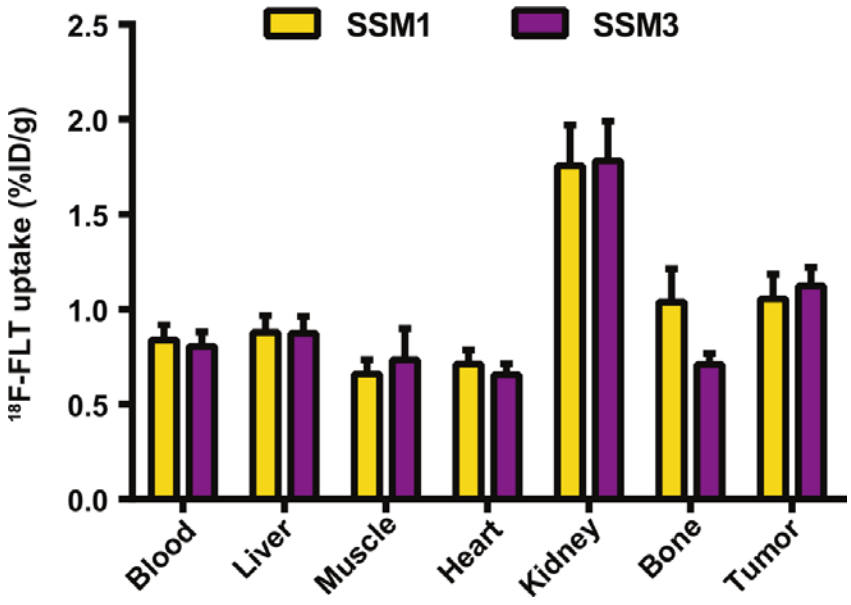


**Supplemental Figure 2: $^{18}$F-FLT biodistribution in STAT1$^{-/-}$ tumor bearing female mice.**

Mice bearing SSM1 tumors (n=4) or SSM3 tumors (n=4) were sacrificed 2 h after injection of 0.85 MBq (23 µCi) $^{18}$F-FLT. Tissues were harvested, weighed, and radioactivity was measured by gamma counting. Percent injected dose/gram (%ID/g) of each tissue type was calculated.